



**HAL**  
open science

# A High Order Method for Contour Integrals with an Application to Plasma Modeling in Nuclear Fusion

Holger Heumann, Lukas Drescher, Kersten Schmidt

► **To cite this version:**

Holger Heumann, Lukas Drescher, Kersten Schmidt. A High Order Method for Contour Integrals with an Application to Plasma Modeling in Nuclear Fusion. [Research Report] RR-8948, INRIA Sophia Antipolis - Méditerranée; CASTOR. 2016. hal-01354031

**HAL Id: hal-01354031**

**<https://inria.hal.science/hal-01354031v1>**

Submitted on 17 Aug 2016

**HAL** is a multi-disciplinary open access archive for the deposit and dissemination of scientific research documents, whether they are published or not. The documents may come from teaching and research institutions in France or abroad, or from public or private research centers.

L'archive ouverte pluridisciplinaire **HAL**, est destinée au dépôt et à la diffusion de documents scientifiques de niveau recherche, publiés ou non, émanant des établissements d'enseignement et de recherche français ou étrangers, des laboratoires publics ou privés.



# A High Order Method for Contour Integrals with an Application to Plasma Modeling in Nuclear Fusion

Holger Heumann, Lukas Drescher, Kersten Schmidt

**RESEARCH  
REPORT**

**N° 8948**

August 17, 2016

Project-Teams CASTOR &  
Institut für Mathematik,  
Technische Universität Berlin,  
Germany

ISRN INRIA/RR--8948--FR+ENG

ISSN 0249-6399





## A High Order Method for Contour Integrals with an Application to Plasma Modeling in Nuclear Fusion

Holger Heumann, Lukas Drescher, Kersten Schmidt

Project-Teams CASTOR & Institut für Mathematik, Technische Universität  
Berlin, Germany

Research Report n° 8948 — August 17, 2016 — 22 pages

**Abstract:** We introduce a novel method to compute approximations of contour integrals. The new method is based on the coarea formula in combination with a Galerkin projection. As such it fits seamlessly into the spirit of hp/spectral finite element methods and circumvents the expensive and technical computation of contours. We provide convergence estimates showing that high order convergence can be achieved provided the data is sufficiently smooth. The theoretical results are supplemented by extensive numerical experiments for an example application from plasma modeling in nuclear fusion.

**Key-words:** contour integrals, high order quadrature, curved interfaces

---

*Address of Holger Heumann* CASTOR, Inria Sophia Antipolis - Méditerranée, 2004, route des Lucioles-BP 93, 06902 Sophia Antipolis Cedex, France

*Address of Lukas Drescher* CASTOR, Inria Sophia Antipolis - Méditerranée, 2004, route des Lucioles-BP 93, 06902 Sophia Antipolis Cedex, France, and Institut für Mathematik, Technische Universität Berlin, Straße des 17. Juni 136, 10623 Berlin, Germany

*Address of Kersten Schmidt* Institut für Mathematik, Technische Universität Berlin, Straße des 17. Juni 136, 10623 Berlin, Germany

**RESEARCH CENTRE  
SOPHIA ANTIPOLIS – MÉDITERRANÉE**

2004 route des Lucioles - BP 93  
06902 Sophia Antipolis Cedex

## **Une Nouvelle Méthode d'ordre élevé pour des Intégrales de surface et curviligne**

**Résumé :** Nous présentons une nouvelle méthode pour calculer des approximations des intégrales de surface et des intégrales curvilignes. Cette méthode est basée sur la formule de co-aire combinée avec une projection de type Galerkin. Elle entre directement dans le cadre des méthodes d'éléments finis d'ordre élevé. Nous démontrons des théorèmes de convergence et les résultats théoriques sont illustrés par des exemples numériques venant d'une application en fusion nucléaire.

**Mots-clés :** intégrale de surface, intégrale de curviligne, intégration numérique, éléments finis d'ordre élevé

# A HIGH ORDER METHOD FOR CONTOUR INTEGRALS WITH AN APPLICATION TO PLASMA MODELING IN NUCLEAR FUSION

HOLGER HEUMANN, LUKAS DRESCHER, AND KERSTEN SCHMIDT

## 1. INTRODUCTION

This article is concerned with the approximation of the integrals

$$(1) \quad g_{f, \bar{\psi}}(y) := \int_{\{\mathbf{x} \in \Omega, \bar{\psi}(\mathbf{x})=y\}} f(\mathbf{x}) \, ds(\mathbf{x}), \quad y \in (0, 1),$$

where  $\bar{\psi} : \Omega \subset \mathbb{R}^n \rightarrow [0, 1]$ ,  $n = 2, 3$  is a Lipschitz continuous, scalar function, and  $f : \Omega \rightarrow \mathbb{R} \cup \{-\infty, \infty\}$  is another integrable scalar function. The values  $g_{f, \bar{\psi}}(y)$  are well defined for all  $y$  for which the sets  $\{\mathbf{x} \in \mathbb{R}^n, \bar{\psi}(\mathbf{x}) = y\}$  are  $(n - 1)$ -dimensional hypersurfaces and  $f$  is bounded on these sets. The functions  $g_{f, \bar{\psi}}$  represent the average of  $f$  over each hypersurface of  $\bar{\psi}$ . In the particular case  $f = 1$  we have that  $g_{f, \bar{\psi}}$  is the area (or length) of the hypersurface. We will assume throughout this work that the area (length)  $g_{1, \bar{\psi}}(y)$  is bounded for almost all  $y \in [0, 1]$ .

If the hypersurfaces of  $\bar{\psi}$  have an explicit parametrization, standard quadrature formulas provide an adequate mean to approximate (1). It is even possible to devise higher order methods that avoid the computation of the derivatives of the parametrization [1].

In here we want to focus on the case where such a parametrization is a priori not known. The standard approach is the following: The scalar functions  $\bar{\psi}$  are approximated by piecewise linear finite element functions  $\bar{\psi}_h$  and the values  $g_{f, \bar{\psi}_h}(y)$  can be assembled from contributions in each element. This approach is a variation of a family of algorithms in computer graphics [25] that are used to visualize hypersurfaces. In the case of linear finite elements this is the *method of marching triangles or tetrahedrons* [26, 30], while projecting onto the bilinear finite element space is the even older *method of marching squares or cubes* [21]. There does not exist, at least to our knowledge, rigorous convergence analysis. But clearly the projection of  $\bar{\psi}$  onto low order spaces restricts the order of the method. Very high accuracy can be only achieved through meshes with a huge number of elements.

It is a well known fact in spectral and higher order methods, that one can find way more economical finite dimensional approximations of  $\bar{\psi}$ , if one exploits properties such as smoothness. Nevertheless we would like to stress that the direct elementwise assembling of  $g_{f, \bar{\psi}_h}$  with  $\bar{\psi}_h$  piecewise polynomials of degree  $p$  will be more difficult and expensive. In the case of linear finite elements the intersections of hypersurfaces with the mesh elements are planar, while in the case of higher order finite elements the intersection are curved. Hence, it is necessary to determine numerically a local parametrization if the accuracy of  $\bar{\psi}_h$  shall be inherited to the approximation of  $g_{f, \bar{\psi}_h}$ . Finding such local parametrizations requires similar techniques as finite element methods on curved domains [7, Chapter 12] and amounts to solve repeatedly non-linear problems. For higher order polynomial approximations of  $\psi$  this approach is fairly expensive and technical. Such efforts might be reasonable if one is interested in values of (1) for one specific value  $y$  as it is the case for

---

*Date:* August 17, 2016,

2010 Mathematics Subject Classification: 65D30, 65N15, 65N30, 76W05

keywords: contour integrals, high order quadrature, curved interfaces.

hypersurface integrals that appear in level set methods and fictitious domain methods or extended finite element methods. A non-exhaustive list of references about this topic is [8, 24, 12] and the many references therein.

In this article we are interested in computing efficiently approximation of (1) on the whole interval  $y \in (0, 1)$ . We propose a novel approach fitting seamlessly into the spirit of higher order finite element methods. We will see that the hypersurface averaging functions (1) are unique solutions of the variational formulation: Seek  $g_{f, \bar{\psi}} \in L^2(0, 1)$  such that

$$(2) \quad \int_0^1 g_{f, \bar{\psi}}(y) \lambda(y) dy = \int_{\Omega} f(\mathbf{x}) |\nabla \bar{\psi}(\mathbf{x})| \lambda(\bar{\psi}(\mathbf{x})) d\mathbf{x} \quad \forall \lambda \in L^2(0, 1).$$

Moreover, we will introduce associated Galerkin methods, where only integrals over the domain  $\Omega$  have to be evaluated.

The main motivation for this work is the magnetohydrodynamic equilibrium equation, an elliptic semi-linear equation for the so-called poloidal flux  $\psi$ . Computing magnetohydrodynamic equilibria is a central problem for modeling of plasma in nuclear fusion reactors. Very important functionals of the solution of such equilibrium problems are the hypersurface averaged quantities (1) that are the focus of this article. In the subsequent section we will adapt the parlance from plasma physics and call the functions (1) the *geometric coefficients*.

The outline of this paper is the following. In the next section, we will recall the coarea formula and show (Lemma 2) that the geometric coefficients verify the weak formulation (2). With this it is straight forward to introduce in Section 3 the Galerkin projection methods to compute approximations of  $g_{f, \bar{\psi}}(y)$  in some finite dimensional space, *e.g.*, a polynomial space. We provide also a convergence estimate that balances a best approximation result and the consistency error. Section 4 presents the plasma equilibrium problem, elaborates on details for computing the geometric coefficients and states a couple of regularity results. Extensive numerical experiments highlight the practicability of the new method.

## 2. GEOMETRIC COEFFICIENTS AND THE COAREA FORMULA

We recall that  $\bar{\psi} : \Omega \subset \mathbb{R}^n \rightarrow (0, 1)$ ,  $n = 2, 3$  is a Lipschitz continuous, scalar function, not necessary monotone and that the geometric coefficients are the integrals

$$g_{f, \bar{\psi}}(y) := \int_{\{\mathbf{x} \in \Omega, \bar{\psi}(\mathbf{x}) = y\}} f(\mathbf{x}) ds(\mathbf{x}),$$

with  $f : \Omega \mapsto \mathbb{R} \cup \{-\infty, \infty\}$  another integrable scalar function. We have the following result, the *coarea formula*, highlighting the relationship between integrated geometric coefficients  $g_{f, \bar{\psi}}(y)$  and volume integrals.

**Theorem 1** (Coarea formula). *Let  $f : \Omega \rightarrow \mathbb{R} \cup \{-\infty, \infty\}$  be integrable and  $\bar{\psi} : \Omega \rightarrow [0, 1]$  Lipschitz, then  $g_{f, \bar{\psi}} \in L^1(0, 1)$  and*

$$\int_0^1 g_{f, \bar{\psi}}(y) dy = \int_{\Omega} f(\mathbf{x}) |\nabla \bar{\psi}(\mathbf{x})| d\mathbf{x}.$$

*Proof.* See [9, Theorem 3.2.12]. □

An immediate corollary of the coarea formula is the following identity.

**Corollary 2.** *Let the assumptions of Theorem 1 be fulfilled. If moreover  $f |\nabla \bar{\psi}|^{\frac{1}{2}} \in L^2(\Omega)$  and  $g_{1, \bar{\psi}} \in L^\infty(0, 1)$  then  $g_{f, \bar{\psi}} \in L^2(0, 1)$  and*

$$(3) \quad \int_0^1 g_{f, \bar{\psi}}(y) \lambda(y) dy = \int_{\Omega} f(\mathbf{x}) \lambda(\bar{\psi}(\mathbf{x})) |\nabla \bar{\psi}(\mathbf{x})| d\mathbf{x} \quad \forall \lambda \in L^2(0, 1).$$

*Proof.* The assertion is an immediate consequence of the obvious identity  $g_{f,\bar{\psi}}(y)\lambda(y) = g_{f,\lambda(\bar{\psi}),\bar{\psi}}(y)$  and Theorem 1, and so

$$\int_0^1 g_{f,\bar{\psi}}(y) \lambda(y) dy = \int_0^1 g_{f,\lambda(\bar{\psi}),\bar{\psi}}(y) dy = \int_{\Omega} f(\mathbf{x}) \lambda(\bar{\psi}(\mathbf{x})) |\nabla \bar{\psi}(\mathbf{x})| d\mathbf{x}.$$

The Cauchy-Schwarz inequality implies

$$\int_{\Omega} f(\mathbf{x}) \lambda(\bar{\psi}(\mathbf{x})) |\nabla \bar{\psi}(\mathbf{x})| d\mathbf{x} \leq \|f\|_{L^2(\Omega)} \|\lambda \circ \bar{\psi}\|_{L^2(\Omega)},$$

and so the right-hand side of (3) is bounded in  $L^2(0, 1)$  due to

$$\begin{aligned} \|\lambda \circ \bar{\psi}\|_{L^2(\Omega)}^2 &= \left| \int_{\Omega} \lambda^2(\bar{\psi}(\mathbf{x})) |\nabla \bar{\psi}(\mathbf{x})| d\mathbf{x} \right| \\ &= \left| \int_0^1 g_{1,\bar{\psi}}(y) \lambda^2(y) dy \right| \leq \|\lambda\|_{L^2(0,1)} \|g_{1,\bar{\psi}}\|_{L^\infty(0,1)}. \end{aligned}$$

Hence, the variational formulation (3) for  $g_{f,\bar{\psi}} \in L^2(0, 1)$  is well-posed and the proof is complete.  $\square$

We are going to use this formula to compute approximations of the geometric coefficients via a Galerkin projection, rather than introducing directly discretizations of (1).

We introduce  $\mathcal{P}_P(0, 1)$  the space of all polynomials of degree less or equal to  $P$  on  $[0, 1]$  and look for an approximation  $g_{f,\bar{\psi}}^P \in \mathcal{P}_P(0, 1)$  of  $g_{f,\bar{\psi}}$  such that

$$(4) \quad \int_0^1 g_{f,\bar{\psi}}^P(y) \lambda(y) dy = \int_0^1 g_{f,\bar{\psi}}(y) \lambda(y) dy \quad \forall \lambda \in \mathcal{P}_P(0, 1),$$

where we have as a standard approximation result [28, Theorem 3.17]

$$(5) \quad \|g_P - g_{f,\bar{\psi}}\|_{L^2(0,1)} \leq \inf_{v \in \mathcal{P}_P(0,1)} \|v - g_{f,\bar{\psi}}\|_{L^2(0,1)} \leq CP^{-k} \|g_{f,\bar{\psi}}\|_{H^k(0,1)},$$

with  $C > 0$ ,  $C \in \mathbb{R}$  independent of  $P$  but dependent of  $k$ . The strength of this idea is that we can use the coarea formula (Corollary 2) to rewrite the integration over  $[0, 1]$  in the right hand side of (4) in an integration over  $\Omega$

$$(6) \quad \int_0^1 g_P(y) \lambda(y) dy = \int_{\Omega} f(\mathbf{x}) \lambda(\bar{\psi}(\mathbf{x})) |\nabla \bar{\psi}| d\mathbf{x} \quad \forall \lambda \in \mathcal{P}_P(0, 1),$$

which, when working with the hp/spectral FEM approximation rather than with  $\psi$ , is our new approach.

**Remark 3** (Continuity of geometric coefficients). *To obtain in general geometric coefficients  $g_{f,\bar{\psi}}$  that are continuous in  $(0, 1)$  and so  $H^k(0, 1)$  regular with  $k \geq \frac{1}{2}$  that can be approximated in  $\mathcal{P}_P(0, 1)$  with a convergence rate larger than  $\frac{1}{2}$  we have to assume that  $\bar{\psi}$  takes almost all values in  $[0, 1]$ . If  $\bar{\psi}$  does not take values in a subinterval  $I \subset (0, 1)$  then the geometric coefficients are zero for all  $y \in I$  and might be discontinuous on  $\partial I$ . In this case the convergence rate would be below  $\frac{1}{2}$ .*

### 3. DISCRETIZATION AND CONVERGENCE

Let  $V_{h,p} \subset C^0(\Omega)$  be a finite element space defined over a triangulation of  $\Omega$ , where  $h > 0$  corresponds to the largest diameter of an element of the triangulation and  $p$  to the polynomial degree on the reference element. In the following we think of  $\bar{\psi}_{h,p} \in V_{h,p}$  as approximation of  $\bar{\psi}$  with  $\bar{\psi}_{h,p} : \Omega \rightarrow [0, 1]$  and we assume standard approximation results

$$\|\bar{\psi} - \bar{\psi}_{h,p}\|_{L^2(\Omega)} \leq Ch^{p+1} \quad \text{and} \quad \|\bar{\psi} - \bar{\psi}_{h,p}\|_{H^1(\Omega)} \leq Ch^p.$$



So  $\bar{\psi}_{h,p}$  can be for example the  $L^2$  or another kind of Galerkin projection of a function  $\bar{\psi}$ . We refer to Sec. 4, where  $\bar{\psi}_{h,p}$  is the scaled to  $(0, 1)$  Galerkin projection of the solution  $\psi$  of a partial differential equation.

We introduce the **Galerkin projection of geometric coefficients**: Find  $g_{f_{h,p}, \bar{\psi}_{h,p}}^P \in \mathcal{P}_P(0, 1)$  such that

$$(7) \quad \int_0^1 g_{f_{h,p}, \bar{\psi}_{h,p}}^P(y) \lambda(y) dy = \int_{\Omega} f_{h,p}(\mathbf{x}) \lambda(\bar{\psi}_{h,p}(\mathbf{x})) |\nabla \bar{\psi}_{h,p}(\mathbf{x})| d\mathbf{x} \quad \forall \lambda \in \mathcal{P}_P(0, 1).$$

We introduced here also  $f_{h,p}(\mathbf{x})$  to cover cases where  $f$  depends on  $\bar{\psi}$  and, hence,  $f_{h,p}$  on its approximation such as  $f(\mathbf{x}) = |\nabla \bar{\psi}(\mathbf{x})|^2$ , where  $f_{h,p}(\mathbf{x})$  will be  $|\nabla \bar{\psi}_{h,p}(\mathbf{x})|^2$ . The implementation of (7) compromises two steps/ingredients. Firstly, a standard  $(P+1) \times (P+1)$  mass matrix containing the  $L^2$  inner products of pairs for basis functions of  $\mathcal{P}_P(0, 1)$  has to be assembled. This mass matrix becomes diagonal when Legendre polynomials – mapped to  $(0, 1)$  – are used as basis functions. Second,  $P+1$  entries of the right hand side vector has to be assembled. As  $\lambda(\bar{\psi})$  is piecewise smooth with respect to the mesh underlying the definition of  $V_{h,p}$ , these  $P+1$  entries can be approximated by the normal quadrature rules in hp/spectral FEM. In particular there is no need to determine explicitly the hypersurfaces of  $\psi_{h,p}$ .

We have the following well-posedness and convergence results, the latter balancing the best approximation error  $\inf_{v \in \mathcal{P}_P(0,1)} \|v - g_{f, \bar{\psi}}\|_{L^2(0,1)}$  with the  $L^2$ -error of  $\bar{\psi}_{h,p}$ .

**Theorem 4** (Well-posedness and error of discretized geometric coefficients). *Let the assumptions of Corollary 2 be fulfilled and let the sets  $\{\mathbf{x} \in \mathbb{R}^n, \bar{\psi}(\mathbf{x}) = y\}$  be  $(n-1)$ -dimensional hypersurfaces for all  $y \in [0, 1]$ . If moreover for  $f_{h,p} : \Omega \rightarrow \mathbb{R} \cup \{-\infty, \infty\}$  and  $\bar{\psi}_{h,p} \in V_{h,p}$  it holds  $f_{h,p} |\nabla \bar{\psi}_{h,p}|^{\frac{1}{2}} \in L^2(\Omega)$  then the solution  $g_{f_{h,p}, \bar{\psi}_{h,p}}^P$  of (7) is well-defined in  $L^2(0, 1)$  and for any  $k > 0$  there exists a constant  $C > 0$  such that*

$$\begin{aligned} \|g_{f_{h,p}, \bar{\psi}_{h,p}}^P - g_{f, \bar{\psi}}\|_{L^2(0,1)} &\leq C (P^{-k} \|g_{f, \bar{\psi}}\|_{H^k(0,1)} + \|(f |\nabla \bar{\psi}| - f_{h,p} |\nabla \bar{\psi}_{h,p}|) |\nabla \bar{\psi}|^{-\frac{1}{2}}\|_{L^2(\Omega)}) \\ &\quad + 8\sqrt{3} P^4 \|\bar{\psi} - \bar{\psi}_{h,p}\|_{L^2(\Omega)} \|f_{h,p} |\nabla \bar{\psi}_{h,p}|\|_{L^2(\Omega)}. \end{aligned}$$

*Proof.* The well-posedness follows from the Lax-Milgram lemma, where the assumption on  $f_{h,p}$  and  $\bar{\psi}_{h,p}$  leads similarly to the proof of Corollary 2 to  $g_{f_{h,p}, \bar{\psi}_{h,p}}^P \in L^2(0, 1)$ .

To prove the estimate on the discretization error we introduce first the notation

$$(f, \lambda \circ \bar{\psi})_{\Omega} = \int_{\Omega} f(\mathbf{x}) \lambda(\bar{\psi}(\mathbf{x})) d\mathbf{x}.$$

Then, the Strang lemma [5, Chap. III] yields

$$\begin{aligned} \|g_{f_{h,p}, \bar{\psi}_{h,p}}^P - g_{f, \bar{\psi}}\|_{L^2(0,1)} &\leq \inf_{\lambda \in \mathcal{P}_P(0,1)} \|\lambda - g_{f, \bar{\psi}}\|_{L^2(0,1)} \\ &\quad + \sup_{\lambda \in \mathcal{P}_P(0,1)} \frac{|(f |\nabla \bar{\psi}|, \lambda \circ \bar{\psi})_{\Omega} - (f_{h,p} |\nabla \bar{\psi}_{h,p}|, \lambda \circ \bar{\psi}_{h,p})_{\Omega}|}{\|\lambda\|_{L^2(\Omega)}} \end{aligned}$$

and we estimate the numerator in the second term on the right hand side:

$$\begin{aligned} &|(f |\nabla \bar{\psi}|, \lambda \circ \bar{\psi})_{\Omega} - (f_{h,p} |\nabla \bar{\psi}_{h,p}|, \lambda \circ \bar{\psi}_{h,p})_{\Omega}| \\ &\leq |(f |\nabla \bar{\psi}| - f_{h,p} |\nabla \bar{\psi}_{h,p}|, \lambda \circ \bar{\psi})_{\Omega}| + |(f_{h,p} |\nabla \bar{\psi}_{h,p}|, \lambda \circ \bar{\psi} - \lambda \circ \bar{\psi}_{h,p})_{\Omega}| \\ &\leq \|(f |\nabla \bar{\psi}| - f_{h,p} |\nabla \bar{\psi}_{h,p}|) |\nabla \bar{\psi}|^{-\frac{1}{2}}\|_{L^2(\Omega)} \| |\nabla \bar{\psi}|^{\frac{1}{2}} (\lambda \circ \bar{\psi}) \|_{L^2(\Omega)} \\ (8) \quad &+ |(f_{h,p} |\nabla \bar{\psi}_{h,p}| \cdot (\bar{\psi} - \bar{\psi}_{h,p}), \lambda' \circ \eta)_{\Omega}| \end{aligned}$$

where we used the Cauchy-Schwarz inequality and the mean value theorem, stating that there is some function  $\eta: \Omega \rightarrow (0, 1)$  such that for all  $\mathbf{x} \in \Omega$

$$\lambda(\bar{\psi}(\mathbf{x})) - \lambda(\bar{\psi}_{h,p}(\mathbf{x})) = \lambda'(\eta(\mathbf{x}))(\bar{\psi}(\mathbf{x}) - \bar{\psi}_{h,p}(\mathbf{x}))$$

and the fact that  $C^\infty(0, 1)$  is dense in  $L^2(0, 1)$ .

Using the Cauchy-Schwarz inequality we can bound the last term in (8) as

$$\begin{aligned} & |(f_{h,p}|\nabla\bar{\psi}_{h,p}| \cdot (\bar{\psi} - \bar{\psi}_{h,p}), \lambda' \circ \eta)_\Omega| \\ & \leq \sup_{y \in (0,1)} |\lambda'(y)| \|f_{h,p}|\nabla\bar{\psi}_{h,p}|\|_{L^2(\Omega)} \|\bar{\psi} - \bar{\psi}_{h,p}\|_{L^2(\Omega)}, \end{aligned}$$

where Sobolev embedding estimates and inverse estimates for polynomials lead to

$$\sup_{y \in (0,1)} |\lambda'(y)| \leq 8\sqrt{3}P^4 \|\lambda\|_{L^2(0,1)}.$$

More precisely, it is easy to verify that the Sobolev embedding estimate [28, Theorem A.21]

$$\|\lambda'\|_{L^\infty(0,1)} \leq \frac{2}{\sqrt{3}} \|\lambda'\|_{H^1(0,1)}$$

holds, and with inverse estimates [28, Theorem 3.91] for  $\lambda \in \mathcal{P}_P(0, 1)$  we find

$$\begin{aligned} \|\lambda'\|_{L^2(0,1)} & \leq 2\sqrt{3}P^2 \|\lambda\|_{L^2(0,1)}, \\ \|\lambda''\|_{L^2(0,1)} & \leq 2\sqrt{3}(P-1)^2 \|\lambda'\|_{L^2(0,1)} \leq 12P^2(P-1)^2 \|\lambda\|_{L^2(0,1)}. \end{aligned}$$

Hence, we can bound

$$\|\lambda'\|_{L^\infty(0,1)}^2 \leq \frac{4}{3} (\|\lambda'\|_{L^2(0,1)}^2 + \|\lambda''\|_{L^2(0,1)}^2) \leq 192 P^8 \|\lambda\|_{L^2(0,1)}^2.$$

Moreover, the assumptions of the theorem on  $f_{h,p}$  and  $\bar{\psi}_{h,p}$  and  $V_{h,p} \subset C^0(\Omega)$  imply  $f_{h,p}|\nabla\bar{\psi}_{h,p}| \in L^2(\Omega)$ . Finally, by the coarea formula (3)

$$\| |\nabla\bar{\psi}|^{\frac{1}{2}} (\lambda \circ \bar{\psi}) \|_{L^2(\Omega)}^2 = (|\nabla\bar{\psi}| \lambda \circ \bar{\psi}, \lambda \circ \bar{\psi})_\Omega = \int_0^1 \lambda^2(y) g_{1,\bar{\psi}}(y) dy.$$

and the assertion follows.  $\square$

**Remark 5.** Our numerical experiments in Section 4 indicate that the high powers of  $P$  in the bound of Theorem 4 are by far too pessimistic.

**Remark 6.** The assumption in Theorem 4, that the sets  $\{\mathbf{x} \in \mathbb{R}^n, \bar{\psi}(\mathbf{x}) = y\}$  are  $(n-1)$ -dimensional hypersurfaces for all  $y \in [0, 1]$  is not very critical. If for  $y_0 \in [0, 1]$  the set  $\{\mathbf{x} \in \mathbb{R}^n, \bar{\psi}(\mathbf{x}) = y_0\}$  is not a  $(n-1)$ -dimensional hypersurface, then the geometric coefficient  $g_{f,\bar{\psi}}$  is infinite at  $y = y_0$ . However, with the assumptions of Corollary 2  $g_{f,\bar{\psi}}$  is bounded in  $L^2(0, 1)$  even so if  $\bar{\psi}$  is constant in each connected component of a  $n$ -dimensional open set  $\Omega_0 \subset \Omega$ . Note, that the term  $\|(f|\nabla\bar{\psi}| - f_{h,p}|\nabla\bar{\psi}_{h,p}|)|\nabla\bar{\psi}|^{-\frac{1}{2}}\|_{L^2(\Omega)}$  in Theorem 4 can be replaced in this case by  $\|(f|\nabla\bar{\psi}| - f_{h,p}|\nabla\bar{\psi}_{h,p}|)|\nabla\bar{\psi}|^{-\frac{1}{2}}\|_{L^2(\Omega \setminus \Omega_0)} + 4P^2 \|f_{h,p}|\nabla\bar{\psi}_{h,p}|\|_{L^1(\Omega_0)}$ .

As a simple corollary, inverse inequalities yield a convergence result for the error of the Galerkin approximation  $g_{f_{h,p},\bar{\psi}_{h,p}}^P$  measured in the  $H^1$ -seminorm and the  $L^\infty$ -norm.

**Theorem 7** ( $H^1$ - and  $L^\infty$ -error of the discretized geometric coefficients). *Let the assumptions of Theorem 4 be fulfilled. Then, for any  $k > 0$ , there exists a constant  $C > 0$  such that*

$$\|g_{f_{h,p},\bar{\psi}_{h,p}}^P - g_{f,\bar{\psi}}\|_{H^1(0,1)} \leq CP^2 \left( \|g_{f_{h,p},\bar{\psi}_{h,p}}^P - g_{f,\bar{\psi}}\|_{L^2(0,1)} + P^{-k} \|g_{f,\bar{\psi}}\|_{H^k(0,1)} \right)$$

and the same bound holds for the error in the  $L^\infty(0, 1)$ -norm.

*Proof.* According to [28, Theorem 3.17] we have a projection operator  $I_P : H^1(0, 1) \rightarrow \mathcal{P}_P(0, 1)$  such that for all  $v \in H^k(0, 1)$

$$\|v - I_P v\|_{H^1(0,1)} \leq CP^{1-k} \|v\|_{H^k(0,1)}, \quad \|v - I_P v\|_{L^2(0,1)} \leq CP^{-k} \|v\|_{H^k(0,1)}.$$

Combining these results with triangle inequalities and inverse inequality [28, Theorem 3.91] we obtain the estimate in the  $H^1$ -seminorm as

$$\begin{aligned} |g_{f_{h,p}, \bar{\psi}_{h,p}}^P - g_{f, \bar{\psi}}|_{H^1(0,1)} &\leq |g_{f_{h,p}, \bar{\psi}_{h,p}}^P - I_P g_{f, \bar{\psi}}|_{H^1(0,1)} + |I_P g_{f, \bar{\psi}} - g_{f, \bar{\psi}}|_{H^1(0,1)} \\ &\leq CP^2 \|g_{f_{h,p}, \bar{\psi}_{h,p}}^P - I_P g_{f, \bar{\psi}}\|_{L^2(0,1)} + CP^{1-k} \|g_{f, \bar{\psi}}\|_{H^k(0,1)} \\ &\leq CP^2 \|g_{f_{h,p}, \bar{\psi}_{h,p}}^P - g_{f, \bar{\psi}}\|_{L^2(0,1)} + CP^{1-k} (1 + P) \|g_{f, \bar{\psi}}\|_{H^k(0,1)}. \end{aligned}$$

The  $L^\infty(0, 1)$ -estimate follows from the Sobolev embedding theorem, e.g. [28, Theorem A.21].  $\square$

**Remark 8.** In the setting of (7) we know for  $\lambda \in \mathcal{P}_P(0, 1)$  and  $\bar{\psi}_{h,p} \in V_{h,p}$  that also the restriction  $\lambda \circ \bar{\psi}_{h,p}|_K$  to an element  $K$  of  $\tau_h$  is the image of a polynomial defined on the reference element, and hence the consistency error due to quadrature falls into the usual setting of variational crimes (see e.g. [19, pp. 155-166] and [6, pp. 201-203]).

**Remark 9.** It is straightforward to replace  $\mathcal{P}_P(0, 1)$  in (7) with some other finite dimensional approximation space, such as spline spaces, for which we can prove a similar convergence results as in the preceding theorem. On the other hand it is a priori not obvious, whether standard quadrature on elements of the mesh  $\tau_h$  underlying the definition of  $V_{h,p}$  is sufficient.

**Remark 10.** If one is only interested in the approximation in specific values of  $g_{f, \bar{\psi}}(y)$ , e.g. at  $y = y_c$ ,  $y_c \in (0, 1)$ , as it would be the case for level set methods, fictitious domain method or extended finite element methods, it might be worth to introduce a smooth window function  $w_\varepsilon : \mathbb{R} \rightarrow \mathbb{R}$  with  $w_\varepsilon(0) = 1$  and compact support  $(-\varepsilon, \varepsilon)$ . Clearly  $g_{f \cdot w_\varepsilon(\bar{\psi} - y_c), \bar{\psi}}(y_c) = g_{f, \bar{\psi}}(y_c)$  and

$$\int_0^1 g_{f \cdot w_\varepsilon(\bar{\psi} - y_c), \bar{\psi}}(y) \lambda(y) dy = \int_\Omega f(\mathbf{x}) w_\varepsilon(\bar{\psi}(\mathbf{x}) - y_c) \lambda(\bar{\psi}(\mathbf{x})) |\nabla \bar{\psi}(\mathbf{x})| d\mathbf{x}.$$

The integrand in the right hand side of the last equation vanishes in large parts of the domain  $\Omega$  which reduces the amount of work required to assemble the right hand side of the Galerkin projection (7). Theorem 7 provides a convergence result.

Alternatively, depending on the application and the concrete setting, it is also possible to pursue a more localized approach, where the global integral  $g_{f, \bar{\psi}}(y)$  is split into a sum of integrals

$$g_{f, \bar{\psi}}(y_c) = \sum_T g_{f, \bar{\psi}}^T(y_c) = \sum_T \int_{\{\mathbf{x} \in \Omega \cap T, \bar{\psi}(\mathbf{x}) = y_c\}} f(\mathbf{x}) ds(\mathbf{x})$$

where the summation runs over the elements  $T$  of a non-overlapping decomposition of  $\Omega$ . Exemplary for this are the fictitious domain methods, where one needs to evaluate integrals  $g_{f, \bar{\psi}}$  for a large number of different  $f$  with local support. Applying our method to the approximation of  $g_{f, \bar{\psi}}^T(y_c)$  replaces the technical integration on exact, but non-polynomial boundaries with quadrature on  $T$ , that is in general readily available. The convergence assertion of Theorems 4 and 7 control the approximation error and in the simplest case of exact  $f$  and  $\bar{\psi}$ , this reduces to the standard error (5) of polynomial approximation in 1D.

#### 4. APPLICATION: THE AXISYMMETRIC PLASMA EQUILIBRIUM PROBLEM

In the following we will consider a continuous, bounded scalar function  $\psi : \Omega \subset \subset (\mathbb{R}_+ \times \mathbb{R}) \rightarrow \mathbb{R}$  and introduce the normalization

$$\bar{\psi}(r, z) = \frac{\psi(r, z) - \psi^0(\psi)}{\psi^1(\psi) - \psi^0(\psi)} \in (0, 1).$$

with  $\psi^1(\psi) = \inf_{(r,z) \in \Omega} \psi(r, z)$ ,  $\psi^0(\psi) := \sup_{(r,z) \in \Omega} \psi(r, z)$ . In our application, the *axisymmetric magnetohydrodynamic equilibrium problem*,  $\psi$  is the so-called poloidal flux and solution to the following elliptic quasi-linear partial differential equation:

$$(9) \quad \begin{aligned} -\nabla \cdot \left( \frac{1}{\mu_0 r} \nabla \psi(r, z) \right) &= j_p(r, \bar{\psi}) \quad \text{in } \Omega; \\ \psi(r, z) &= \psi_{\text{bd}} \quad \text{at } \partial\Omega; \end{aligned}$$

with  $\psi_{\text{bd}} \in \mathbb{R}$ ,  $\nabla$  the gradient in two dimensions and  $\mu_0$  the constant magnetic permeability of vacuum. The right hand side  $j_p(r, \bar{\psi})$  is supposed to be known and positive, but in general non-linear in  $\bar{\psi}$ . Hence, by the maximum principle we have  $\psi^1 = \inf_{x \in \Omega} \psi(x) = \psi_{\text{bd}}$ . The equation (9) is the celebrated Grad-Shafranov-Schlüter equation [15, 29, 22], that is one of the central equations for modeling of magnetically confined plasma in tokamaks. The domain  $\Omega$  corresponds to a section through the torus-shaped domain covered by the plasma in the tokamak and it can be easily shown that (9) is the equilibrium problem of magnetohydrodynamics (MHD) in systems with axial symmetry. The MHD equilibrium is the combination of magnetostatics

$$\text{curl } \mathbf{B} = \mu_0 \mathbf{J}, \quad \text{div } \mathbf{B} = 0$$

and force balance

$$\text{grad } p = \mathbf{J} \times \mathbf{B}$$

with  $\mathbf{B}$  the magnetic induction,  $\mathbf{J}$  the electric current density and  $p$  the hydrodynamic pressure. The source term  $j_p$  and  $\psi/r$  in (9) are the axial components of  $\mathbf{J}$  and  $\mathbf{A}$ , where  $\mathbf{A}$  is the electric vector potential with  $\mathbf{B} = \text{curl } \mathbf{A}$ . We refer to standard text books [11, 4, 13, 18] for the details of the derivation. While (9) is usually referred to as the *fixed-boundary equilibrium problem* as  $\Omega$  is fixed, there is also the even more important *free-boundary equilibrium problem* that is formulated in an unbounded domain with boundary conditions at infinity and where the domain covered by the plasma is an unknown. Clearly, the numerical solution of free-boundary equilibrium problems faces more difficulties [16] than the fixed-boundary equilibrium problem. But as the focus of this work is the approximation of the geometric coefficients we restrict the presentation to the fixed-boundary equilibrium problem while remarking that our new approach to compute geometric coefficients generalizes with minor modifications to the free-boundary equilibrium problem.

In the famous Grad/Hogan-approach [15, 14, 17] the transient MHD equations are reformulated as the so-called coupled problem of equilibrium and resistive diffusion and transport equations. While the equilibrium problem is the one we introduced in (9), the resistive diffusion and transport equations are basically Faraday's law and the hydrodynamic equations written in the curvi-linear coordinate system that is induced by the contour lines of the poloidal flux function  $\psi$ . The variation along the flux lines is neglected and the geometric coefficients

$$(10) \quad c_{f, \bar{\psi}}(y) = \int_{\{(r,z) \in \Omega, \bar{\psi}(r,z)=y\}} \frac{f(r, z)}{|\nabla \bar{\psi}(r, z)|} r ds$$

that appear due to this coordinate transformation are related to the coefficients (1) for  $n = 2$ ,  $ds(\mathbf{x}) = r ds$  and  $d\mathbf{x} = r dr dz$  via

$$g_{f, \bar{\psi}}(y) = c_{f, |\nabla \bar{\psi}|, \bar{\psi}}(y).$$

The unknowns of the resistive diffusion and transport equation on the other hand determine in some non-linear fashion the profile of the current density  $j_p$  in the equilibrium problem (9). Due to the unusual non-linear coupling the equations in the Grad/Hogan-approach were dubbed *queer differential equations*. The Grad/Hogan-approach is the method of choice, when it comes to the simulation of plasma evolution on the longest timescale, the timescale of resistive diffusion, where entire discharge scenarios can be modeled. Devising stable algorithms is very challenging and an active area of research with many open problems. Numerical methods for computing accurately not only the geometric coefficients but also sensitivities are an important step towards stable and efficient methods for the coupled problem.

**4.1. Galerkin formulation.** We introduce the spaces

$$\begin{aligned} V &:= \{\psi : \Omega \rightarrow \mathbb{R}, \|\psi\|_{L^2(\Omega)} < \infty, \|\nabla\psi\|_{L^2(\Omega)} < \infty\} \cap C^0(\Omega) \\ V_0 &:= \{\psi \in V, \psi|_{\partial\Omega} = 0\} \end{aligned}$$

with

$$\|\psi\|_{L^2(\Omega)}^2 = \int_{\Omega} \psi^2 r^{-1} dr dz$$

and the mappings  $A : V \times V \rightarrow \mathbb{R}$  and  $J_p : V \times V \rightarrow \mathbb{R}$  with

$$(11) \quad A(\psi, \xi) := \int_{\Omega} \frac{1}{\mu_0 r} \nabla\psi \cdot \nabla\xi dr dz \quad \text{and} \quad J_p(\psi, \xi) := \int_{\Omega} j_p(r, \bar{\psi}) \xi dr dz.$$

Then, we have the weak formulation of (9): find  $\psi - \psi^1 \in V_0$  such that

$$(12) \quad A(\psi, \xi) = J_p(\psi, \xi), \quad \forall \xi \in V_0.$$

In the general non-linear case it is convenient to use Newton's method to solve the non-linear problem: the Newton update  $\psi^{n+1}$  is the solution of the infinite dimensional linear system

$$A(\psi^{n+1}, \xi) - D_{\psi} J_p(\psi^n, \xi)(\psi^{n+1}) = J_p(\psi^n, \xi) + D_{\psi} J_p(\psi^n, \xi)(\psi^n), \quad \forall \xi \in V_0.$$

The derivative of  $J_p$  follows from [4, Lemma I.4]:

$$(13) \quad \begin{aligned} D_{\psi} J_p(\psi, \xi)(\tilde{\psi}) &= \int_{\Omega} \frac{\partial j_p(r, \bar{\psi})}{\partial \psi_N} \frac{\bar{\psi} \xi}{\psi^1 - \psi^0(\psi)} dr dz, \\ &+ \tilde{\psi}(r_0(\psi), z_0(\psi)) \int_{\Omega} \frac{\partial j_p(r, \bar{\psi})}{\partial \bar{\psi}} \frac{1 - \bar{\psi}}{\psi^1 - \psi^0(\psi)} \xi dr dz. \end{aligned}$$

We have implemented the Galerkin method for (12) in CONCEPTS [10, 27, 34] (`www.concepts.math.ethz.ch`), using finite dimensional  $hp$ -FEM approximation spaces  $V_{h,p}$  for  $V$ . CONCEPTS is a  $hp$ -FEM library that is based on basis functions defined on rectangular reference domains. Transfinite interpolation techniques ensure that boundaries of the mapped reference elements coincide with the (curved) boundaries of the domain.

For the most general case rigorous theoretical convergence results are not yet available, mainly due the  $j_p$  depending on the normalized poloidal flux. If  $j_p$  is independent of the normalized poloidal flux  $\bar{\psi}$  we end up with a linear problem and have the usual convergence assertion.

**Theorem 11.** *Let  $\psi$  be the solution of (12) and  $\psi_{h,p} \in \psi_{h,p} \in V_{h,p} \cap V_0$  the solution of its Galerkin discretization satisfying*

$$(14) \quad A(\psi_{h,p}, \xi) = J_p(\psi_{h,p}, \xi) + A(\psi^1, \xi), \quad \forall \xi \in V_{h,p} \cap V_0.$$

For  $j_p(r, \bar{\psi})$  independent of  $\bar{\psi}$  we have

$$\|\psi - \psi_{h,p}\|_{L^2(\Omega)} \leq Ch^{p+1} \quad \text{and} \quad \|\psi - \psi_{h,p}\|_{H^1(\Omega)} \leq Ch^p.$$

with constants  $C > 0$  independent of  $h$  and  $p$ .

Moreover we have the pointwise estimates for any  $\mathbf{x} \in \Omega$

$$(15) \quad (\psi - \psi_{h,p})(\mathbf{x}) \leq C \begin{cases} h^{p+1} \log(h^{-1}) & p = 1 \\ h^{p+1} & p > 1 \end{cases}.$$

*Proof.* Convergence estimates in  $L^2$  and  $H^1$  are standard. The pointwise estimate follow as in [33, Theorem 11.1]  $\square$

The **Galerkin projection of geometric coefficients** for this application is: Find  $c_{f_{h,p}, \bar{\psi}_{h,p}}^P \in \mathcal{P}_P(0, 1)$  such that

$$(16) \quad \int_0^1 c_{f_{h,p}, \bar{\psi}_{h,p}}^P(y) \lambda(y) dy = \int_{\Omega} f_{h,p}(r, z) \lambda(\bar{\psi}_{h,p}(r, z)) r dr ds \quad \forall \lambda \in \mathcal{P}_P(0, 1).$$

Similar as in Theorem 4 we can deduce a convergence result, that balances in this case the best approximation error  $\inf_{v \in \mathcal{P}_P(0,1)} \|v - c_{f, \bar{\psi}}\|_{L^2(0,1)}$  with the  $L^2$ -error of  $\psi_{h,p}$  and the error of the maximal  $\psi_{h,p}$ -value.

**Theorem 12.** *Let the assumptions of Corollary 2 be fulfilled, let the sets  $\{\mathbf{x} \in \mathbb{R}^n, \bar{\psi}(\mathbf{x}) = y\}$  be  $(n - 1)$ -dimensional hypersurfaces for all  $y \in [0, 1]$  and  $\psi_{h,p}$  be the solution of (14) that converges pointwise to  $\psi$  the solution of (12). If moreover for  $f_{h,p} : \Omega \rightarrow \mathbb{R} \cup \{-\infty, \infty\}$  and  $\bar{\psi}_{h,p} \in V_{h,p}$  it holds  $f_{h,p} |\nabla \bar{\psi}_{h,p}|^{-\frac{1}{2}} \in L^2(\Omega)$  then the solution  $c_{f_{h,p}, \bar{\psi}_{h,p}}^P$  of (16) is well-defined in  $L^2(0, 1)$  and for any  $k > 0$  there exists a constant  $C > 0$  such that, asymptotically,*

$$\begin{aligned} \|c_{f_{h,p}, \bar{\psi}_{h,p}}^P - c_{f, \bar{\psi}}\|_{L^2(0,1)} &\leq C(P^{-k} \|c_{f, \bar{\psi}}\|_{H^k(0,1)} + \|f - f_{h,p}\|_{L^2(\Omega)}) \\ &\quad + CP^4 \|\psi - \psi_{h,p}\|_{L^\infty(\Omega)}. \end{aligned}$$

*Proof.* From Theorem 4 we have

$$\begin{aligned} \|c_{f_{h,p}, \bar{\psi}_{h,p}}^P - c_{f, \bar{\psi}}\|_{L^2(0,1)} &\leq C(P^{-k} \|c_{f, \bar{\psi}}\|_{H^k(0,1)} + \|f - f_{h,p}\|_{L^2(\Omega)}) \\ &\quad + CP^4 \|\bar{\psi} - \bar{\psi}_{h,p}\|_{L^2(\Omega)}. \end{aligned}$$

We note

$$\begin{aligned} \|\bar{\psi} - \bar{\psi}_{h,p}\|_{L^2(\Omega)} &\leq \left\| \frac{\psi - \psi_{h,p} + \psi^0(\psi) - \psi^0(\psi_{h,p})}{\psi^1 - \psi^0(\psi)} \right\|_{L^2(\Omega)} \\ &\quad + \left| \frac{\psi^1(\psi_{h,p}) - \psi^0(\psi_{h,p})}{\psi^1 - \psi^0(\psi)} - 1 \right| \|\bar{\psi}_{h,p}\|_{L^2(\Omega)}, \end{aligned}$$

from which we have

$$\begin{aligned} &\left( 1 - \left| \frac{\psi^1(\psi_{h,p}) - \psi^0(\psi_{h,p})}{\psi^1 - \psi^0(\psi)} - 1 \right| \right) \|\bar{\psi} - \bar{\psi}_{h,p}\|_{L^2(\Omega)} \leq \\ &\left( \left\| \frac{\psi - \psi_{h,p} + \psi^0(\psi) - \psi^0(\psi_{h,p})}{\psi^1 - \psi^0(\psi)} \right\|_{L^2(\Omega)} + \left| \frac{\psi^1(\psi_{h,p}) - \psi^0(\psi_{h,p})}{\psi^1 - \psi^0(\psi)} - 1 \right| \|\bar{\psi}\|_{L^2(\Omega)} \right). \end{aligned}$$

As for  $h$  small enough or  $p$  large enough

$$\left| \frac{\psi^1(\psi_{h,p}) - \psi^0(\psi_{h,p})}{\psi^1 - \psi^0(\psi)} - 1 \right| < 1,$$

we conclude

$$\|\bar{\psi} - \bar{\psi}_{h,p}\|_{L^2(\Omega)} \leq C(\|\psi - \psi_{h,p}\|_{L^2(\Omega)} + |\psi^0(\psi) - \psi^0(\psi_{h,p})|) \leq C\|\psi - \psi_{h,p}\|_{L^\infty(\Omega)},$$

and the assertions follow.  $\square$

**Remark 13.** *The high powers of  $P$  in the bound of Theorem 12 are a consequence of the estimates of Theorem 4. Once again, our numerical experiments in Section 4 indicate they are too pessimistic.*

Again we can deduce a convergence result for the error measured in the  $H^1$ -norm.

**Theorem 14.** *Let the assumptions of Theorem 12 be fulfilled. Then, for any  $k > 0$ , there exists a constant  $C > 0$  such that*

$$|c_{f_{h,p}, \bar{\psi}_{h,p}}^P - c_{f, \bar{\psi}}|_{H^1(0,1)} \leq CP^{1-k}(1+P)\|c_{f, \bar{\psi}}\|_{H^k(0,1)} + CP^2\|c_{f_{h,p}, \bar{\psi}_{h,p}}^P - c_{f, \bar{\psi}}\|_{L^2(0,1)}.$$

**4.2. Sensitivities of geometric coefficients.** In many practical application it is useful to compute not only the geometric coefficients but also the sensitivities with respect to the poloidal flux map  $\psi$  in some direction  $\delta\psi$ :

$$(17) \quad \langle D_\psi c_{f, \bar{\psi}}(y), \delta\psi \rangle = \lim_{\varepsilon \rightarrow 0} \frac{c_{f, \bar{\psi} + \varepsilon \delta\psi}(y) - c_{f, \bar{\psi}}(y)}{\varepsilon}.$$

Examples are Newton-type methods for the coupled problem of equilibrium and resistive diffusion and transport. Similarly, in optimization problems for the coupled problem such sensitivities are required.

By the coarea formula we find as in Corollary 2 the following characterization of the sensitivities of the geometric coefficients:

$$(18) \quad \int_0^1 \langle D_\psi c_{f, \bar{\psi}}(y), \delta\psi \rangle \lambda(y) dy = L_{f, \psi}(\lambda, \delta\psi) \quad \forall \lambda \in L^2(0, 1),$$

with

$$L_{f, \psi}(\lambda, \delta\psi) = \int_\Omega f(r, z) \lambda'(\bar{\psi}(r, z)) \frac{\delta\psi(r, z)}{\psi^1(\psi) - \psi^0(\psi)} r dr dz - \int_\Omega f(r, z) \lambda'(\bar{\psi}(r, z)) \frac{1 - \bar{\psi}(r, z)}{\psi^1(\psi) - \psi^0(\psi)} \delta\psi(r_0(\psi), z_0(\psi)) r dr dz,$$

where we used the non-trivial derivative

$$D_\psi \psi^0(\psi)(\delta\psi) = \delta\psi(r_0(\psi), z_0(\psi)).$$

The functional  $(r_0(\psi), z_0(\psi)) = \arg \sup_{(r,z) \in \Omega} \psi(r, z)$  is the location of the supremum.

Likewise as for the geometric coefficients we have a simple Galerkin method for computing approximations of the sensitivities.

**Galerkin projection of sensitivities of geometric coefficients** Find  $Dc_{f_{h,p}, \psi_{h,p}}^P(\delta\psi_{h,p}) \in \mathcal{P}_P(0, 1)$  such that

$$(19) \quad \int_0^1 Dc_{f_{h,p}, \psi_{h,p}}^P(\delta\psi_{h,p})(y) \lambda(y) dy = L_{\hat{f}, \psi_{h,p}}(\lambda, \delta\psi_{h,p}) \quad \forall \lambda \in L^2(0, 1).$$

And again the method can be implement with standard quadrature rules on elements of the mesh underlying the definition of  $V_{h,p}$ . If the same quadrature rules are used on (7) and (19), then the discretization of the continuous sensitivity is identical to the sensitivity of the discretization of the geometric coefficient. This will be different, when free-boundary problems are considered and we refer to [16] for the details on quadrature and sensitivities for intersection of triangles and level sets.

**4.3. A few regularity results for geometric coefficients.** The assumption  $c_{f,\bar{\psi}} \in H^k(0, 1)$  in Theorem 4 is fairly strong, seen the definition (10). First of all it seems to be obvious that  $c_{f,\bar{\psi}}$  loses regularity in the neighborhood of values  $y \in [0, 1]$  where  $\psi$  attains a critical point. Second, we know that solutions of elliptic problems in non-smooth domains lose regularity in the vicinity of corners of the boundary of the domain and it can be expected that this loss of regularity influences the regularity of the geometric coefficients. While precise characterization of the regularity of solutions of the non-linear elliptic problem (9) in domains with corners can be found in [2, 3], all the test cases and examples in fusion engineering literature are arbitrarily smooth. Moreover it is an open problem how the regularity of  $\psi$  influences the regularity of  $c_{f,\bar{\psi}}$ . There is also very few theory available explaining how critical points of  $\psi$  influence the regularity of  $c_{f,\bar{\psi}}$ . The only result, we are aware of, is due to G. Vigfusson, stated without proof in [32, Theorem 2].

**Theorem 15** (G. Vigfusson 1979). *Assume that  $\psi$  has only one critical point, that is the maximum of  $\psi$  in  $\Omega$  and  $\psi|_{\partial\Omega} \equiv \psi^1 \in \mathbb{R}$ , then*

$$c_{f,\bar{\psi}} \in C^n([0, 1]), \quad \text{if } f \in C^{2n}(\Omega) \text{ and } \bar{\psi} \in C^{2n+2}(\Omega).$$

*Proof.* The proof for  $n = 0$  and  $n = 1$  follows from various results in [31] and is based on a technique called *elliptic expansions* that compares the contour lines of  $\bar{\psi}$  with ellipses and quantifies the deviation. The Theorems 9 and 10 in [31, p. 62] provide

$$(20) \quad C_{1,\bar{\psi}}(\cdot) := \int_0^1 c_{1,\bar{\psi}}(y') dy' \in C^{n+1}([0, 1]) \quad \text{if } \bar{\psi} \in C^{2n+2}(\Omega),$$

with  $n = 0, n = 1$  or  $n = 2$ . Furthermore, another theorem in [31, p. 75] states

$$(21) \quad \frac{c_{f,\bar{\psi}}}{c_{1,\bar{\psi}}} \in C^n([0, 1]), \quad \text{if } f \in C^{2n}(\Omega) \text{ and } \bar{\psi} \in C^{2n+1}(\Omega),$$

with  $n = 0$  or  $n = 1$  and the assertion of Theorem 15 follows.  $\square$

Such a smoothness result is not true if  $\psi$  has saddle points in  $\Omega$  as we see for the example in the following remark.

**Remark 16.** *We consider  $\Omega = [0, 1]^2$ ,  $\bar{\psi}(r, z) = 1 - rz$  and  $f(r, z) = \sum_{i,j \geq 0} a_{ij} r^i z^j$  with  $a_{ij} \in \mathbb{R}$ .  $\bar{\psi}(r, z)$  has a saddle point at  $(r_X, z_X) = (0, 0)$  with  $y_X = 1$ . We compute for  $f_1(r, z) = r^n z^m$ ,  $n, m \in \mathbb{N}$ ,  $n \neq m$ :*

$$\begin{aligned} C_{f_1,\bar{\psi}}(y) &= \int_{1-y}^1 \left( \int_{(1-y)/z}^1 r^n z^m dr \right) dz \\ &= \frac{(m-n) - (m+1)(1-y)^{n+1} + (n+1)(1-y)^{m+1}}{(m+1)(n+1)(m-n)} \end{aligned}$$

and for  $f_2(r, z) = r^n z^n$ ,  $n \in \mathbb{N}$ :

$$\begin{aligned} C_{f_2,\bar{\psi}}(y) &= \int_{1-y}^1 \left( \int_{(1-y)/z}^1 r^n z^n dr \right) dz \\ &= \frac{1 - (1-y)^{n+1}}{(n+1)^2} + \frac{(1-y)^{n+1} \log(1-y)}{n+1}, \end{aligned}$$

which yields

$$C'_{f_1,\bar{\psi}}(y) = c_{f_1,\bar{\psi}}(y) = \frac{(1-y)^n - (1-y)^m}{m-n}.$$

and

$$C'_{f_2,\bar{\psi}}(y) = c_{f_2,\bar{\psi}}(y) = -\log(1-y)(1-y)^n.$$



Hence we find

$$c_{f,\bar{\psi}}(y) = \sum_{i,j \geq 0, i \neq j} a_{ij} \frac{(1-y)^i - (1-y)^j}{j-i} - \log(1-y) \sum_{i \geq 0} a_{ii} (1-y)^i.$$

In the neighborhood of the saddle point  $y = y_X (= 1)$  the geometric coefficients  $c_{f,\bar{\psi}}(y)$  behave like  $\log(y_X - y)$  whenever  $a_{00} \neq 0$ . In particular,  $c_{f,\bar{\psi}}(y_X)$  is unbounded, while the quotient  $c_{f,\bar{\psi}}(y_X)/c_{1,\bar{\psi}}(y_X)$  is bounded:

$$\lim_{y \rightarrow y_X} \frac{c_{f,\bar{\psi}}(y)}{c_{1,\bar{\psi}}(y)} = f(r_X, z_X) = a_{00}.$$

**4.4. Numerical Experiment: Elliptic Equilibrium.** We consider an elliptic equilibrium described by

$$(22) \quad \psi_E(r, z) = \psi^0 - \left( \frac{(r-r_0)^2}{a^2} + \frac{(z-z_0)^2}{b^2} \right),$$

with  $\psi^1 = 0$ . We have an explicit parametrization for the iso-surfaces:

$$\left\{ \begin{pmatrix} r \\ z \end{pmatrix} ; \psi(r, z) = s \right\} = \left\{ \begin{pmatrix} r_E(t) \\ z_E(t) \end{pmatrix} = \begin{pmatrix} r_0 + a\sqrt{\psi^0 - s} \cos(t) \\ z_0 + b\sqrt{\psi^0 - s} \sin(t) \end{pmatrix} ; 0 \leq t \leq 2\pi \right\}.$$

and the right hand side for the Grad-Shafranov equation (9) evaluates to:

$$-\nabla \cdot \left( \frac{1}{\mu_0 r} \nabla \psi_E(r, z) \right) = \frac{1}{\mu_0} \left( \frac{2}{a^2 r} + \frac{2}{b^2 r} - \frac{2(r-r_0)}{a^2 r^2} \right).$$

In the subsequent calculations we are using always  $\psi_0 = 2$ ,  $(r_0, z_0) = (2, 0)$  and  $a = 1$ ,  $b = 3$ .

**4.4.1. Convergence of  $\psi_E$ .** To begin with we are using the Galerkin method (12) to determine an approximation  $\psi_{h,p}$  of  $\psi_E$  in  $V_{h,p}$ . As this example case is linear the standard analysis for elliptic problems asserts convergence estimates

$$(23) \quad \|\psi_E - \psi_{h,p}\|_{L^2(\Omega)} = O(h^{p+1}) \quad \text{and} \quad \|\psi_E - \psi_{h,p}\|_{H^1(\Omega)} = O(h^p),$$

which are clearly reproduced by our experiments (see Figure 4.4.1).

**4.4.2. Convergence of the the geometric coefficients.** Moving on to the geometric coefficients we find using

$$\begin{aligned} |\nabla \psi_E|^2 &= (\psi^0 - s)(b^2 \cos(t)^2 + a^2 \sin(t)^2) \frac{4}{a^2 b^2}, \\ \dot{r}_E(t)^2 + \dot{z}_E(t)^2 &= (\psi^0 - s)(b^2 \cos(t)^2 + a^2 \sin(t)^2), \end{aligned}$$

the following analytic values

$$\begin{aligned} c_{\frac{1}{r^2}, \bar{\psi}_E}(y) &= \int_{\bar{\psi}_E=y} \frac{r^{-1}}{|\nabla \bar{\psi}_E|} ds = \int_0^{2\pi} \frac{\sqrt{\dot{r}(t)^2 + \dot{z}(t)^2}}{r(t) |\nabla \bar{\psi}_E|} dt = \frac{|\psi^0| ab\pi}{\sqrt{r_0^2 + a^2 \psi^0 y}} \\ c_{\frac{|\nabla \psi_E|^2}{r^2}, \bar{\psi}_E}(y) &= |\psi^0| \int_{\bar{\psi}_E=y} \frac{|\nabla \psi_E|}{r} ds = \int_0^{2\pi} \frac{\sqrt{\dot{r}(t)^2 + \dot{z}(t)^2}}{|\nabla \bar{\psi}_E|} \frac{|\nabla \psi_E|^2}{r} dt = \\ &= 4\pi |\psi^0| \frac{(b^2 - a^2)r_0(r_0 - \sqrt{r_0^2 + a^2 \psi^0 y}) - a^4 \psi^0 y}{a^3 b \sqrt{r_0^2 + a^2 \psi^0 y}}. \end{aligned}$$

Fixing the polynomial degree  $P$  of approximation of the geometric coefficients the Theorems 12 and 14 assert

$$\left\{ \begin{aligned} \|c_{f_{h,p}, \bar{\psi}_{h,p}}^P - c_{f,\bar{\psi}}\|_{L^2(0,1)} \\ \|c_{f_{h,p}, \bar{\psi}_{h,p}}^P - c_{f,\bar{\psi}}\|_{H^1(0,1)} \end{aligned} \right\} = \begin{cases} O(h^{p+1} \log(h^{-1})) & p = 1 \\ O(h^{p+1}) & p > 1 \end{cases},$$

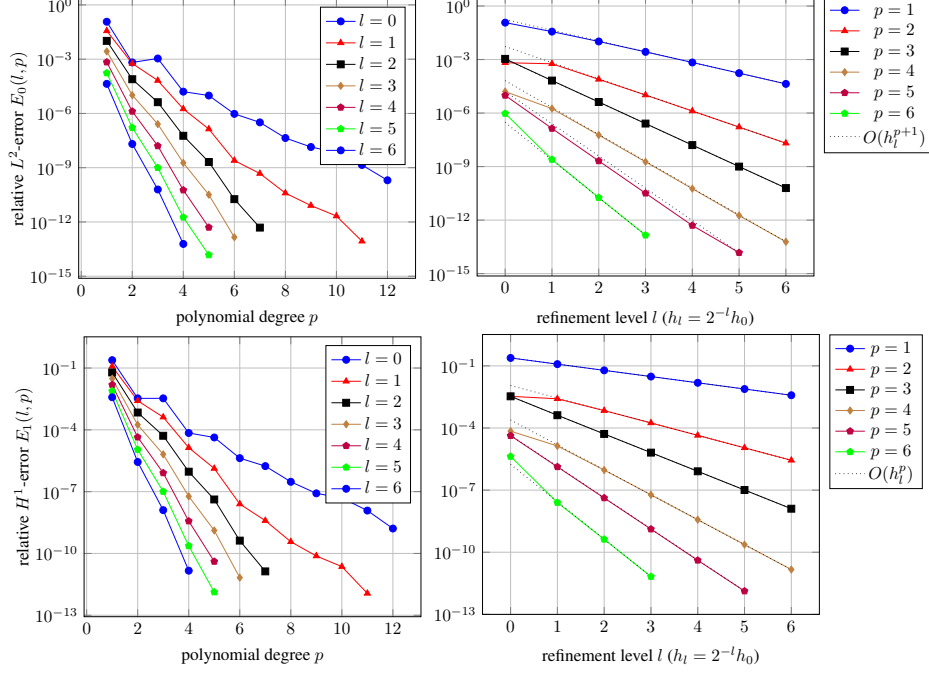


FIGURE 1. Elliptic equilibrium: Relative  $L^2$ -error  $E_0(l, p) := \|\psi_{h_l, p} - \psi_E\|_{L^2(\Omega)} / \|\psi_E\|_{L^2(\Omega)}$  (top) and relative  $H^1$ -error  $E_1(l, p) := \|\psi_{h_l, p} - \psi_E\|_{H^1(\Omega)} / \|\psi_E\|_{H^1(\Omega)}$  (bottom) for refinement in polynomial degree  $p$  (left) and refinement level  $l$  of the mesh (right).

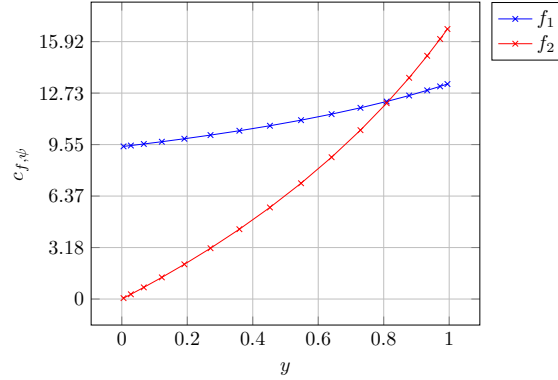


FIGURE 2. Elliptic Equilibrium: Sketch of the geometric coefficients  $c_{f, \psi_E}$  with  $f = f_1 = 1/r^2$  and  $f = f_2 = |\nabla\psi|^2/r^2$ .

for the Galerkin projection  $c_{f_{h,p}, \bar{\psi}_{h,p}}^P$  with  $f_{h,p} = f = 1/r^2$  and

$$\left. \begin{aligned} & \|c_{f_{h,p}, \bar{\psi}_{h,p}}^P - c_{f, \bar{\psi}}\|_{L^2(0,1)} \\ & \|c_{f_{h,p}, \bar{\psi}_{h,p}}^P - c_{f, \bar{\psi}}\|_{H^1(0,1)} \end{aligned} \right\} = O(h^p),$$

with  $f = |\nabla\psi|^2/r^2$  and  $f_{h,p} = |\nabla\psi_{h,p}|^2/r^2$ .

In the following experiments we fix  $P = 15$ . The convergence for  $c_{\frac{1}{r^2}, \bar{\psi}_E}$  is in general better than predicted by Theorem (12) (see Figure 3), when the polynomial degree is larger than 1. The experimental convergence rates seem to indicate that it might be possible to

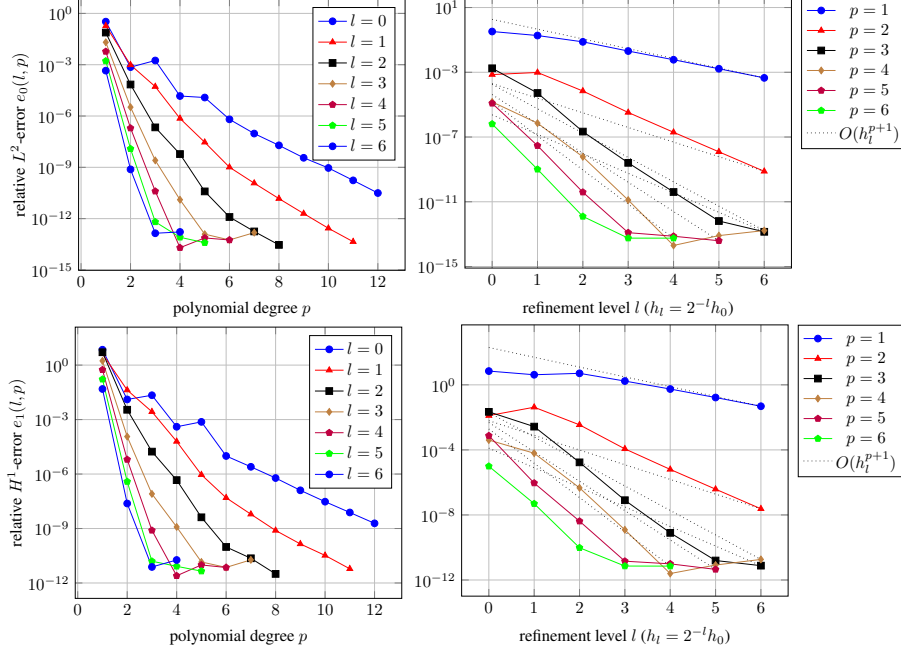


FIGURE 3. Elliptic equilibrium: Relative  $L^2$ -error  $e_0(l, p) := \|c_{f, \psi_{h_l, p}}^P - c_{f, \psi_E}\|_{L^2(0,1)} / \|c_{f, \psi_E}\|_{L^2(0,1)}$  and  $H^1$ -error  $e_1(l, p) := \|c_{f, \psi_{h_l, p}}^P - c_{f, \psi_E}\|_{H^1(0,1)} / \|c_{f, \psi_E}\|_{H^1(0,1)}$  for  $f = 1/r^2$  for refinement in polynomial degree  $p$  (left) and refinement level  $l$  of the mesh (right) with  $P = 15$ .

improve the assertion of Theorem (12) by a duality argument: The experimental rate of convergence for refinement in the mesh for fixed polynomial degree  $p > 2$  seems to be twice as large as predicted by our theory. Moreover (see Figure 5), also for  $c_{\frac{|\nabla \psi_E|^2}{r^2}, \bar{\psi}_E}$  the convergence is better than predicted and except for the lowest order case the additional consistency error due to  $f_{h,p}$  does not seem to spoil the rate of convergence.

The experimental results for the error measured in the  $H^1$ -norm (see Figures 3 and 5) highlights even more that our new method for computing the geometric coefficients is most powerful, when combined with high order polynomial approximation of  $\psi$ . In this case the approximation error in  $\psi$  decays very quickly and the positive powers of  $P$  in front of this approximation error in Theorems (12) and (14) do not harm too much.

Finally, our experiments suggest (see Figures 4 and 6) also that the high powers of the discretization parameter  $P$  in the estimates of Theorem 12 and 14 are too pessimistic. We observe in these examples a convergence like  $P^{\frac{1}{2}}$  rather than  $P^4$  for the error in  $L^2(0, 1)$ . For the error in  $H^1(0, 1)$  we see a convergence like  $P^{\frac{5}{2}}$  rather than  $P^6$ . Additionally we see in the experiments the saturation levels for small  $P$  which highlight that the discretization parameter  $P$  needs to be balanced accordingly with  $h$  and  $p$ , to achieve a desired accuracy level with minimal effort.

**4.5. Numerical Experiment: Solov'ev Equilibrium.** The next example, taken from [23], is a very popular benchmarking case in computational plasma physics. We take

$$\psi_S(r, z) = -\frac{\kappa}{2r_0^3 q_0} \left( \frac{1}{4}(r^2 - r_0^2)^2 + \frac{1}{\kappa^2} r^2 z^2 - a^2 r_0^2 \right)$$

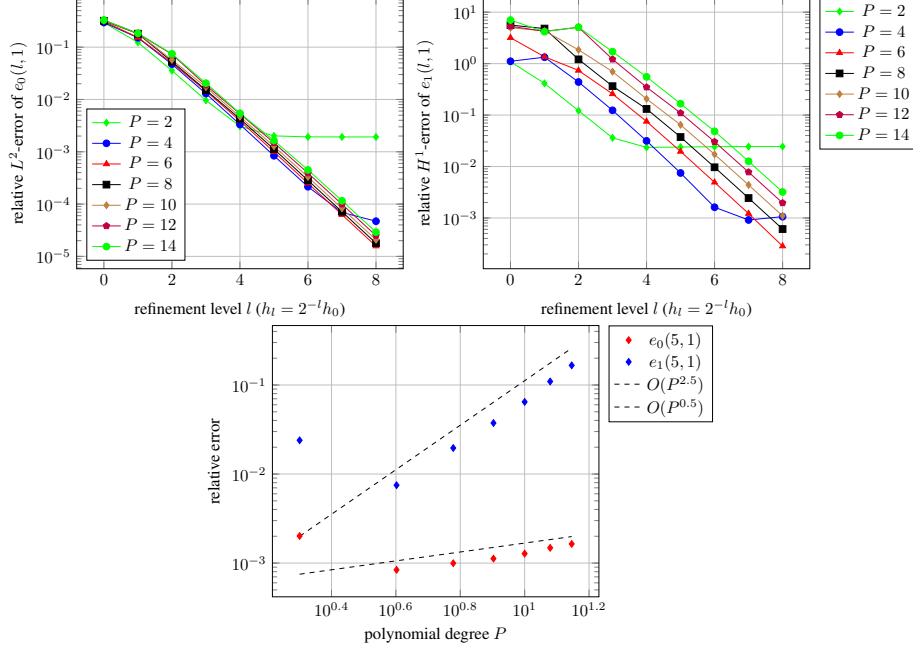


FIGURE 4. Elliptic equilibrium: Relative  $L^2$ -error  $e_0(l, 1) := \|c_{f,\psi_{h_{l,1}}}^P - c_{f,\psi_E}\|_{L^2(0,1)} / \|c_{f,\psi_E}\|_{L^2(0,1)}$  (top left) and  $H^1$ -error  $e_1(l, 1) := \|c_{f,\psi_{h_{l,1}}}^P - c_{f,\psi_E}\|_{H^1(0,1)} / \|c_{f,\psi_E}\|_{H^1(0,1)}$  (top right) for  $f = 1/r^2$  for refinement in polynomial degree  $P$  and refinement level  $l$  of the mesh and relative  $L^2$ -error  $e_0(l, 1)$  and  $H^1$ -error  $e_1(l, 1)$  at fixed level  $l = 5$  for refinement in polynomial degree  $P$  (bottom).

such that it is the solution to (9) with right hand side

$$j_P(r, \bar{\psi}_S) = \frac{1 + \kappa^2}{\mu_0 \kappa r_0^3 q_0} r$$

where  $r_0$  and  $q_0$  are the major radius and the safety factor at the magnetic axis, and  $a$  and  $\kappa$  are the effective minor radius and elongation of the last closed flux surface, given by  $\psi = 0$ . A parametrization of the boundary is

$$\partial\Omega = \{(r, z) : r^2 = r_0^2 + 2ar_0 \cos(t), z = \kappa a \frac{r_0}{r} \sin(t), 0 \leq t \leq 2\pi\}$$

In the following example we will chose the same parameter values  $r_0 = 1$ ,  $a = 0.32$ ,  $\kappa = 1.7$  and  $q_0 = 1.0$  as in [20].

4.5.1. *Convergence of  $\psi_S$ .* As in the case of the elliptic equilibrium our experiments (see Figure 7) reproduce the theoretical convergence results (23). The numerical solutions for the first 3 mesh refinements are shown in Figure 8.

4.5.2. *Convergence of the geometric coefficients.* For this example we do not have analytic values of the various geometric coefficients  $c_{f,\psi}$  with  $f = 1/r^2$  and  $f = |\nabla\psi|^2/r^2$ . Hence, we explore the convergence behavior using a reference  $c_{f,\psi_S}^{\text{ref}} := c_{f,\psi_{h_2,16}}^{15}$  computed at a discretization with  $P = 15$  for the 1D space and  $p = 16$  for the 2D space on the mesh of level  $l = 2$ .

Here again we observe spectral convergence for geometric coefficients  $c_{f,\psi}$  that involve weighting functions  $f$  independent of  $\psi$  (see Figure 10) or weighting functions that are dependent of  $\psi$  (see Figure 11).

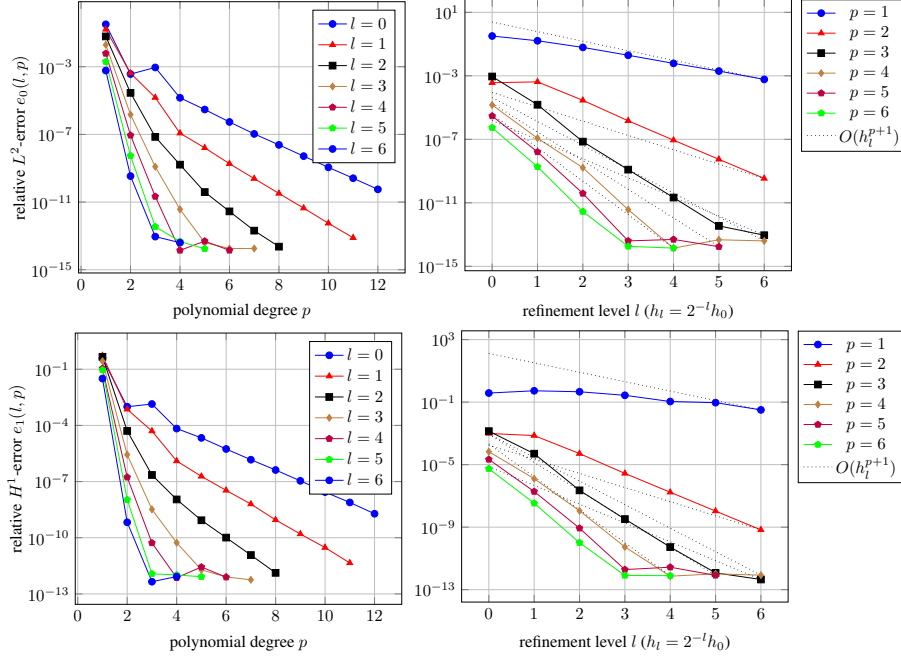


FIGURE 5. Elliptic equilibrium: Relative  $L^2$ -error  $e_0(l, p) := \|c_{f_{h_l, p}, \psi_{h_l, p}}^P - c_{f, \psi_E}\|_{L^2(0,1)} / \|c_{f, \psi_E}\|_{L^2(0,1)}$  and  $H^1$ -error  $e_1(l, p) := \|c_{f_{h_l, p}, \psi_{h_l, p}}^P - c_{f, \psi_E}\|_{H^1(0,1)} / \|c_{f, \psi_E}\|_{H^1(0,1)}$  for  $f = |\nabla \psi_E|^2 / r^2$  and  $f_{h_l, p} = |\nabla \psi_{h_l, p}|^2 / r^2$  for refinement in polynomial degree  $p$  (left) and refinement level  $l$  of the mesh (right) with  $P = 15$ .

## REFERENCES

- [1] K. Atkinson and E. Venturino. Numerical evaluation of line integrals. *SIAM J. Numer. Anal.*, 30(3):882–888, 1993.
- [2] E. Beretta and M. Vogelius. An inverse problem originating from magnetohydrodynamics. II. The case of the Grad-Shafranov equation. *Indiana Univ. Math. J.*, 41(4):1081–1118, 1992.
- [3] E. Beretta and M. Vogelius. An inverse problem originating from magnetohydrodynamics. III. Domains with corners of arbitrary angles. *Asymptotic Anal.*, 11(3):289–315, 1995.
- [4] J. Blum. *Numerical simulation and optimal control in plasma physics*. Wiley/Gauthier-Villars, 1989.
- [5] Dietrich Braess. *Finite Elements: Theory, Fast Solvers, and Applications in Solid Mechanics*. Cambridge University Press, 3th edition, 2007.
- [6] P. G. Ciarlet. Basic error estimates for elliptic problems. In *Handbook of numerical analysis, Vol. II*, Handb. Numer. Anal., II, pages 17–351. North-Holland, Amsterdam, 1991.
- [7] L. Demkowicz. *Computing with hp-adaptive finite elements. Vol. 1*. Chapman & Hall/CRC Applied Mathematics and Nonlinear Science Series. Chapman & Hall/CRC, Boca Raton, FL, 2007. One and two dimensional elliptic and Maxwell problems, With 1 CD-ROM (UNIX).
- [8] Björn Engquist, Anna-Karin Tornberg, and Richard Tsai. Discretization of Dirac delta functions in level set methods. *J. Comput. Phys.*, 207(1):28–51, 2005.
- [9] H. Federer. *Geometric measure theory*. Die Grundlehren der mathematischen Wissenschaften, Band 153. Springer-Verlag New York Inc., New York, 1969.

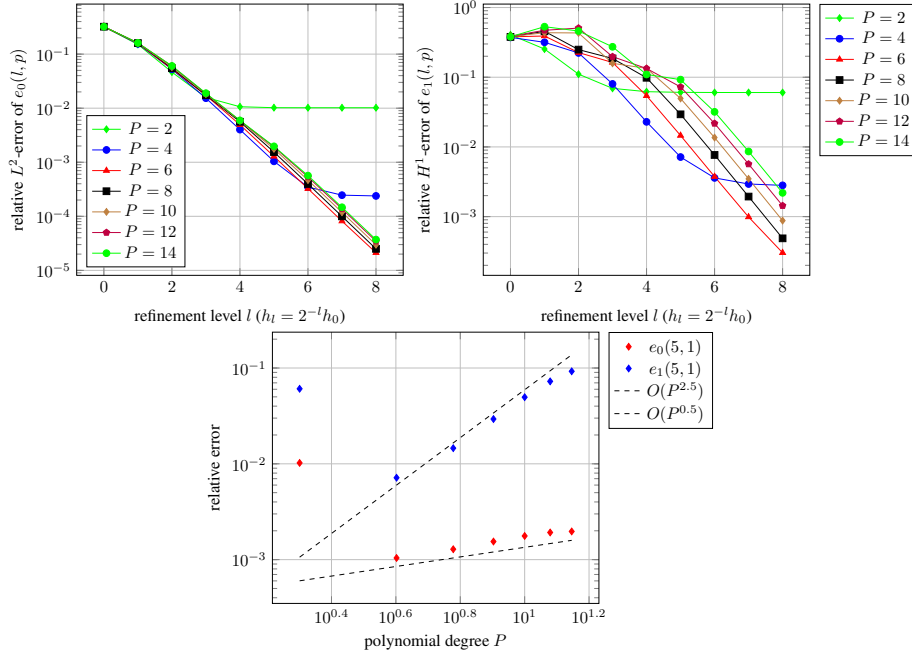


FIGURE 6. Elliptic equilibrium: Relative  $L^2$ -error  $e_0(l, 1) := \|c_{f, \psi_{h_{l,1}}}^P - c_{f, \psi_E}\|_{L^2(0,1)} / \|c_{f, \psi_E}\|_{L^2(0,1)}$  (top left) and  $H^1$ -error  $e_1(l, 1) := \|c_{f, \psi_{h_{l,1}}}^P - c_{f, \psi_E}\|_{H^1(0,1)} / \|c_{f, \psi_E}\|_{H^1(0,1)}$  (top right) for  $f = |\nabla \psi_E|^2 / r^2$  and  $f_{h_{l,p}} = |\nabla \psi_{h_{l,p}}|^2 / r^2$  for refinement in polynomial degree  $P$  and refinement level  $l$  of the mesh and relative  $L^2$ -error  $e_0(l, 1)$  and  $H^1$ -error  $e_1(l, 1)$  at fixed level  $l = 5$  for refinement in polynomial degree  $P$  (bottom).

- [10] Ph. Frauenfelder and Ch. Lage. Concepts – An Object-Oriented Software Package for Partial Differential Equations. *ESAIM: Math. Model. Numer. Anal.*, 36(5):937–951, September 2002.
- [11] J. P. Freidberg. *Ideal Magnetohydrodynamics*. Plenum US, 1987.
- [12] Thomas-Peter Fries and Samir Omerovic. Higher-order accurate integration of implicit geometries. *Internat. J. Numer. Methods Engrg.*, 106(5):323–371, 2016. nme.5121.
- [13] J. P. Goedbloed and S. Poedts. *Principles of magnetohydrodynamics: with applications to laboratory and astrophysical plasmas*. Cambridge university press, 2004.
- [14] H. Grad and J. Hogan. Classical diffusion in a tokamak. *Phys. Rev. Lett.*, 24:1337–1340, Jun 1970.
- [15] H. Grad and H. Rubin. Hydromagnetic equilibria and force-free fields. *Proceedings of the 2nd UN Conf. on the Peaceful Uses of Atomic Energy*, 31:190, 1958.
- [16] H. Heumann, J. Blum, C. Boulbe, B. Faugeras, G. Selig, J.-M. Ané, S. Brémond, V. Grandgirard, P. Hertout, and E. Nardon. Quasi-static free-boundary equilibrium of toroidal plasma with CEDRES++: Computational methods and applications. *Journal of Plasma Physics*, 81, 6 2015.
- [17] F. L. Hinton and R. D. Hazeltine. Theory of plasma transport in toroidal confinement systems. *Rev. Mod. Phys.*, 48:239–308, Apr 1976.
- [18] S. C. Jardin. *Computational methods in plasma physics*. Boca Raton, FL : CRC Press/Taylor & Francis, 2010.

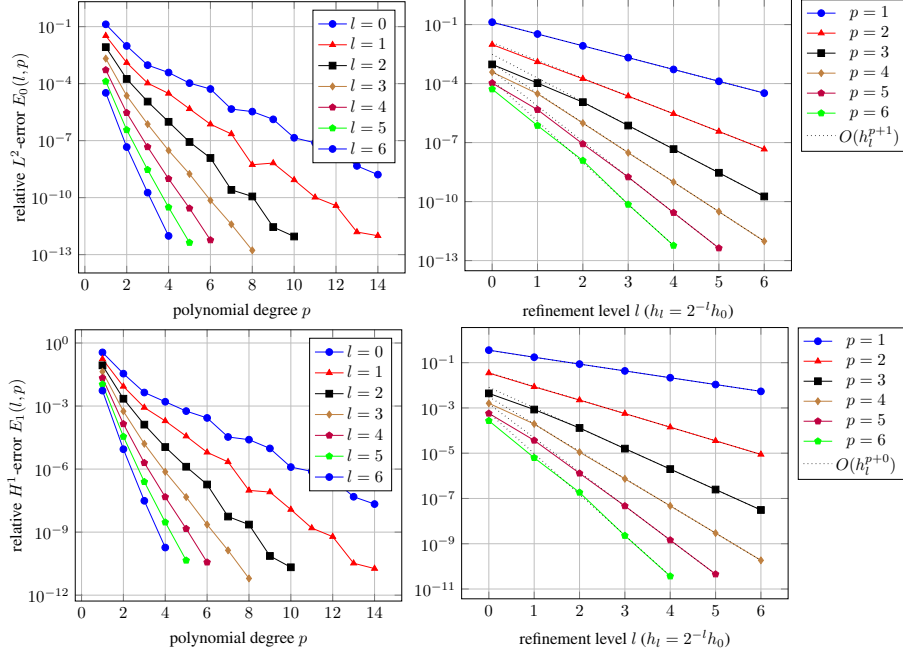


FIGURE 7. Solov'ev Equilibrium: Relative  $L^2$ -error  $E_0(l, p) := \|\psi_{h_l, p} - \psi_S\|_{L^2(\Omega)} / \|\psi_S\|_{L^2(\Omega)}$  (top) and relative  $H^1$ -error  $E_1(l, p) := \|\psi_{h_l, p} - \psi_S\|_{H^1(\Omega)} / \|\psi_S\|_{H^1(\Omega)}$  (bottom) for refinement in polynomial degree  $p$  (left) and refinement level  $l$  of the mesh ( $h_l = 2^{-l}h_0$ ) (right).

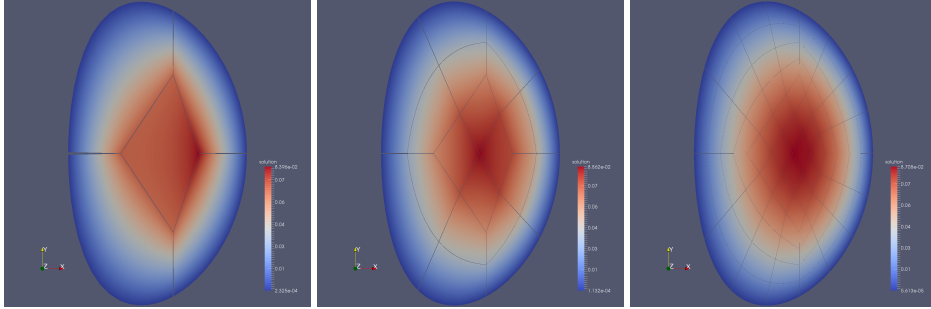


FIGURE 8. Solov'ev equilibrium: The numerical solution for the first 3 mesh refinements.

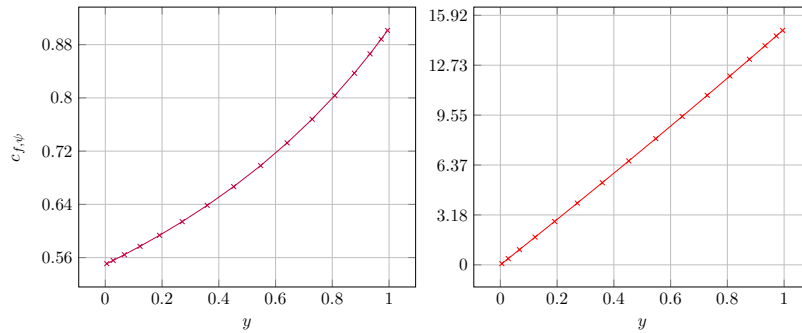


FIGURE 9. Solov'ev equilibrium: Sketch of the geometric coefficients  $c_{f, \psi_S}$  with  $f = f_1 = 1/r^2$  (Left) and  $f = f_2 = |\nabla\psi|^2/r^2$  (Right).

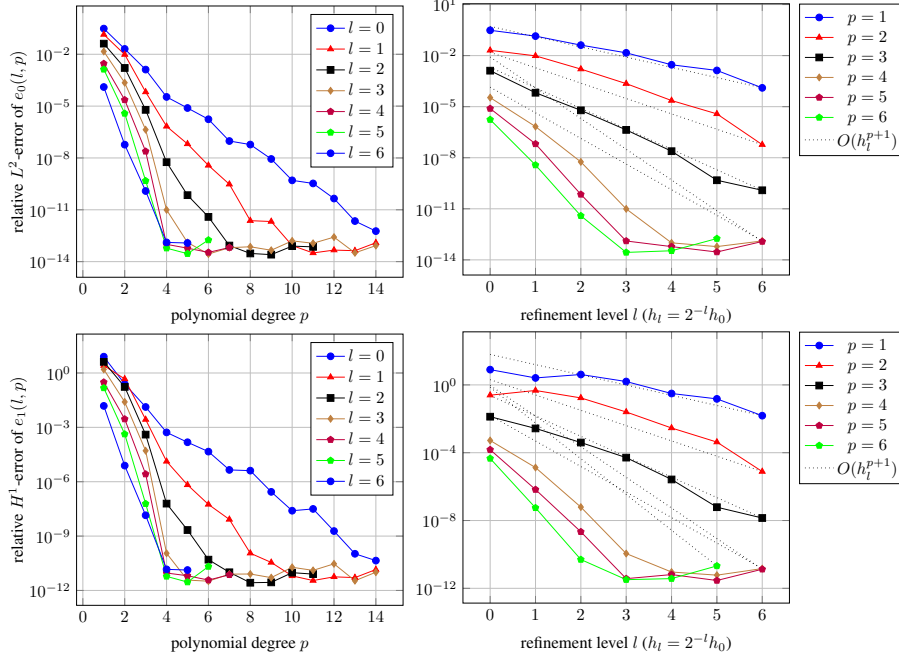


FIGURE 10. Solov'ev equilibrium: Relative  $L^2$ -error  $e_0(l, p) := \|c_{f, \psi_{h_l, p}}^P - c_{f, \psi_S}^{\text{ref}}\|_{L^2(0,1)} / \|c_{f, \psi_S}^{\text{ref}}\|_{L^2(0,1)}$  and  $H^1$ -error  $e_1(l, p) := \|c_{f, \psi_{h_l, p}}^P - c_{f, \psi_S}^{\text{ref}}\|_{H^1(0,1)} / \|c_{f, \psi_S}^{\text{ref}}\|_{H^1(0,1)}$  for  $f = 1/r^2$  for refinement in polynomial degree  $p$  (left) and refinement level  $l$  of the mesh (right) with  $P = 15$ .

- [19] P. Knabner and L. Angermann. *Numerical methods for elliptic and parabolic partial differential equations*, volume 44 of *Texts in Applied Mathematics*. Springer-Verlag, New York, 2003.
- [20] J. Lee and A. Cerfon. Ecom: A fast and accurate solver for toroidal axisymmetric MHD equilibria. *Comput. Phys. Commun.*, 190(0):72 – 88, 2015.
- [21] W. E. Lorensen and H. E. Cline. Marching cubes: A high resolution 3d surface construction algorithm. *SIGGRAPH Comput. Graph.*, 21(4):163–169, August 1987.
- [22] R. Lüst and A. Schlüter. Axialsymmetrische magnetohydrodynamische Gleichgewichtskonfigurationen. *Z. Naturforsch. A*, 12:850–854, 1957.
- [23] H. Lütjens, A. Bondeson, and O. Sauter. The CHEASE code for toroidal MHD equilibria. *Comput. Phys. Commun.*, 97(3):219 – 260, 1996.
- [24] Chohong Min and Frédéric Gibou. Geometric integration over irregular domains with application to level-set methods. *J. Comput. Phys.*, 226(2):1432 – 1443, 2007.
- [25] T. S. Newman and H. Yi. A survey of the marching cubes algorithm. *Computers & Graphics*, 30(5):854 – 879, 2006.
- [26] B. A. Payne and A. W. Toga. Surface mapping brain function on 3d models. *IEEE Computer Graphics and Applications*, 10(5):33–41, Sept 1990.
- [27] Kersten Schmidt and Peter Kauf. Computation of the band structure of two-dimensional photonic crystals with  $hp$  finite elements. *Comput. Methods Appl. Mech. Engrg.*, 198:1249–1259, March 2009.
- [28] C. Schwab.  *$p$ - and  $hp$ -finite element methods : theory and applications in solid and fluid mechanics*. Oxford : Clarendon Press, 2004.
- [29] V. D. Shafranov. On magnetohydrodynamical equilibrium configurations. *Soviet Journal of Experimental and Theoretical Physics*, 6:545, 1958.



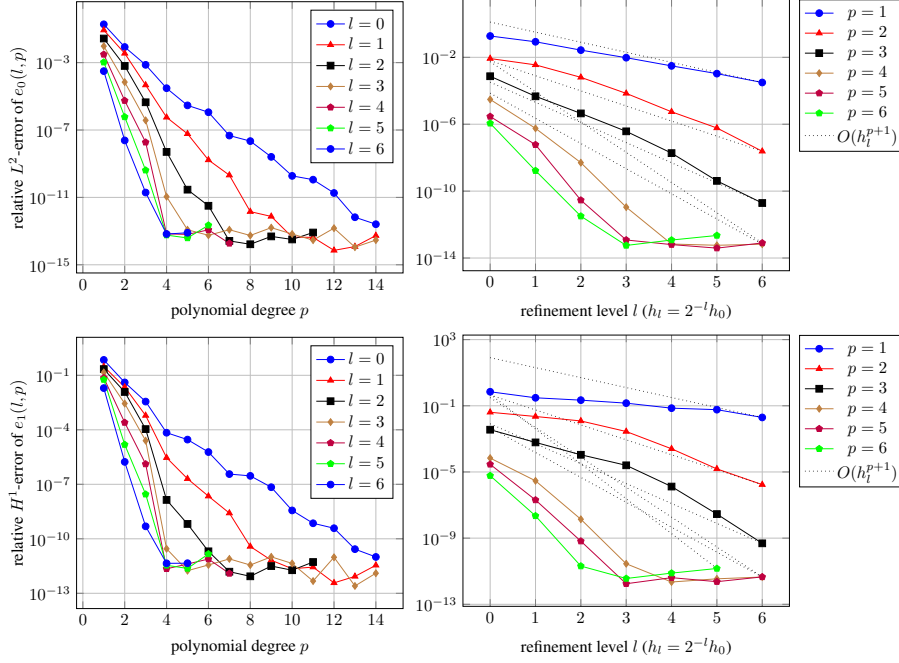


FIGURE 11. Solov'ev equilibrium: Relative  $L^2$ -error  $e_0(l, p) := \|c_{f, \psi_{h_l, p}}^P - c_{f, \psi_S}^{\text{ref}}\|_{L^2(0,1)} / \|c_{f, \psi_S}^{\text{ref}}\|_{L^2(0,1)}$  and  $H^1$ -error  $e_1(l, p) := \|c_{f, \psi_{h_l, p}}^P - c_{f, \psi_S}^{\text{ref}}\|_{H^1(0,1)} / \|c_{f, \psi_S}^{\text{ref}}\|_{H^1(0,1)}$  for  $f = |\nabla \psi_S|^2 / r^2$  and  $f_{h_l, p} = |\nabla \psi_{h_l, p}|^2 / r^2$  for refinement in polynomial degree  $p$  (left) and refinement level  $l$  of the mesh (right) with  $P = 15$ .

- [30] P. Shirley and A. Tuchman. A polygonal approximation to direct scalar volume rendering. *SIGGRAPH Comput. Graph.*, 24(5):63–70, November 1990.
- [31] G. Vigfússon. *The averaged Green function with applications to quasi-static plasma equilibrium*. PhD thesis, New York University, 1977.
- [32] G. Vigfússon. The queer differential equations for adiabatic compression of plasma. *Bull. Amer. Math. Soc. (N.S.)*, 1(5):778–781, 1979.
- [33] L. B. Wahlbin. Local behavior in finite element methods. In *Finite Element Methods (Part 1)*, volume 2 of *Handbook of Numerical Analysis*, pages 353 – 522. Elsevier, 1991.
- [34] Mengyu Wang, Christian Engström, Kersten Schmidt, and Christian Hafner. On high-order FEM applied to canonical scattering problems in plasmonics. *J. Comput. Theor. Nanosci.*, 8:1–9, 2011.

Address of Holger Heumann CASTOR, INRIA SOPHIA ANTIPOLIS - MÉDITERRANÉE, 2004, ROUTE DES LUCIOLES-BP 93, 06902 SOPHIA ANTIPOLIS CEDEX, FRANCE

Address of Lukas Drescher CASTOR, INRIA SOPHIA ANTIPOLIS - MÉDITERRANÉE, 2004, ROUTE DES LUCIOLES-BP 93, 06902 SOPHIA ANTIPOLIS CEDEX, FRANCE, AND INSTITUT FÜR MATHEMATIK, TECHNISCHE UNIVERSITÄT BERLIN, STRASSE DES 17. JUNI 136, 10623 BERLIN, GERMANY

Address of Kersten Schmidt INSTITUT FÜR MATHEMATIK, TECHNISCHE UNIVERSITÄT BERLIN, STRASSE DES 17. JUNI 136, 10623 BERLIN, GERMANY



**RESEARCH CENTRE  
SOPHIA ANTIPOLIS – MÉDITERRANÉE**

2004 route des Lucioles - BP 93  
06902 Sophia Antipolis Cedex

Publisher  
Inria  
Domaine de Voluceau - Rocquencourt  
BP 105 - 78153 Le Chesnay Cedex  
[inria.fr](http://inria.fr)

ISSN 0249-6399